forests

MDPI

Article

Vegetation Mapping and Scenario Simulation in the Poyang Lake Basin of China

Lingjing Wang [1,2], Zemeng Fan [1,2,3,*], Saibo Li [1,2], Yonghui Yao [1,2,3], Zhengping Du [1] and Xuyang Bai [1,2]

[1] State Key Laboratory of Resources and Environment Information System, Institute of Geographical Sciences and Natural Resources Research, Chinese Academy of Sciences, Beijing 100101, China; wanglingjing0027@igsnrr.ac.cn (L.W.); lisb.18s@igsnrr.ac.cn (S.L.); yaoyh@lreis.ac.cn (Y.Y.); duzp@lreis.ac.cn (Z.D.); baixy.20s@igsnrr.ac.cn (X.B.)
[2] College of Resources and Environment, University of Chinese Academy of Sciences, Beijing 100049, China
[3] Jiangsu Center for Collaborative Innovation in Geographical Information Resource Development and Application, Nanjing 210023, China
* Correspondence: fanzm@lreis.ac.cn

Abstract: Climate change has significantly altered plant habitats within the Earth's surface system, reshaping the global distribution and succession of vegetation. The spatiotemporal simulation of vegetation dynamics is essential for effective ecosystem management and conservation at regional scales. In this study, an improved method is developed to analyze the vegetation patterns and scenarios in the Poyang Lake basin, based on the High-Accuracy Surface Modeling (HASM) method and the improved Holdridge Life Zone (HLZ) ecosystem model. HASM is applied to generate high-resolution (250 m × 250 m) spatial grid data for key climate parameters, including mean annual biotemperature (MAB), total annual precipitation (TAP), and potential evapotranspiration ratio (PER), for each decade from 1961 to 2050. The distribution thresholds of vegetation types are calculated based on current vegetation data, MAB, TAP, PER, longitude, latitude, and elevation datasets. In the improved HLZ ecosystem model, the classification parameters of vegetation types have been expanded from three to six. The simulation results indicate that cultivated vegetation, subtropical coniferous forest, and subtropical grassland are the dominant vegetation types, accounting for 75.88% of the total area. Between 2020 and 2050, subtropical coniferous forest is projected to experience the greatest decrease in area, shrinking by an average of 2.65×10^3 km^2 per decade. In contrast, subtropical evergreen–deciduous broadleaf mixed forest is expected to undergo the largest increase, expanding by an average of 1.96×10^3 km^2 per decade. Vegetation types in high-altitude regions exhibit the most rapid changes, with an average decadal variation of 15.26%, whereas low-altitude regions show relatively slower changes, averaging 0.52% per decade. Overall, subtropical grassland, subtropical coniferous forest, and subtropical evergreen–deciduous broadleaf mixed forest in the Poyang Lake basin demonstrate high sensitivity to projected climate change scenarios.

Keywords: vegetation type; spatial pattern; dynamic change; climate change; scenario analysis

check for updates

Academic Editor: Runguo Zang

Received: 12 February 2025
Revised: 26 February 2025
Accepted: 26 February 2025
Published: 27 February 2025

Citation: Wang, L.; Fan, Z.; Li, S.; Yao, Y.; Du, Z.; Bai, X. Vegetation Mapping and Scenario Simulation in the Poyang Lake Basin of China. *Forests* **2025**, *16*, 430. https://doi.org/10.3390/f16030430

Copyright: © 2025 by the authors. Licensee MDPI, Basel, Switzerland. This article is an open access article distributed under the terms and conditions of the Creative Commons Attribution (CC BY) license (https://creativecommons.org/licenses/by/4.0/).

1. Introduction

Climate change has direct, widespread, and long-lasting impacts on the structure and functioning of ecosystems globally [1–3]. It drives shifts in biological communities, influences human living environments, and constrains socio-economic development [4]. Vegetation is a critical component of terrestrial ecosystems, facilitating the exchange of matter and energy between organic and inorganic systems while providing essential habitats

for various organisms [5,6]. In the context of global change, understanding vegetation dynamics and their responses to climate change is fundamental to elucidating the interactions between global change and terrestrial ecosystems [7]. Variations in climatic conditions, such as temperature, precipitation, and solar radiation [8], significantly influence the spatial distribution, composition, and structural characteristics of vegetation. Consequently, examining how key climatic factors affect the spatiotemporal distribution of vegetation and simulating future scenarios represent a pivotal scientific challenge in global change research [9].

Among the numerous studies on vegetation and climate, vegetation ecosystem models have garnered considerable attention from scholars in geography, botany, climatology, and ecology. By analyzing long-term historical climate data, this study aims to elucidate the mechanisms underlying the interactions between climatic factors and vegetation ecosystem changes [10–13]. Incorporating global climate model scenario data allows for effective simulation of climate change characteristics and spatial variations [14], providing insights into future vegetation ecosystem responses. These models enable the simulation and prediction of potential ecosystem changes driven by climate change [15]. Over the past few decades, diverse vegetation models have been developed to simulate spatial distribution patterns, ecological processes, and ecosystem functions under various climatic conditions [16]. Prominent models include the Holdridge Life Zone (HLZ) model [17], BOX model [18], DOLY model [19], MAPSS model [20], BIOME series models [21–24], and IBIS model [25]. The HLZ ecosystem model, in particular, quantitatively classifies vegetation ecosystem types based on three key bioclimatic factors: annual mean biotemperature, annual precipitation, and potential evapotranspiration ratio. With its relatively simple yet robust parameterization, the HLZ model effectively captures the interactions between climate and vegetation, making it widely applicable in environmental assessments, ecological zoning, and predicting the impacts of global change on vegetation ecosystems [26–29].

The Poyang Lake basin, characterized by its complex ecological environment and rich biodiversity, plays a critical role in maintaining the ecological security of the middle and lower reaches of the Yangtze River [30]. It also serves as a cornerstone for the sustainable development of the region's economy, society, and ecology. Against the backdrop of global climate change, the basin holds significant strategic importance as a key area for the "Mountains-Rivers-Lakes" integrated development strategy and the ecological economic initiatives surrounding Poyang Lake, supported at both national and local levels. Simulating the spatiotemporal changes in vegetation types and distribution patterns within the Poyang Lake basin is essential for the protection, restoration, and management of China's integrated ecosystems, encompassing mountains, rivers, forests, farmland, lakes, and grasslands.

Since the 1980s, domestic researchers have conducted extensive studies on the vegetation ecosystems of the Poyang Lake basin. For instance, the spatial distribution and trends of vegetation changes in the Poyang Lake floodplain were analyzed by investigating the relationship between wetland vegetation and environmental factors [31]. By employing the normalized difference vegetation index (NDVI) dataset and meteorological station data, the researchers examined the response of vegetation cover to precipitation in the Poyang Lake basin from 1982 to 1999 at both intra-annual and inter-annual scales [32]. Additionally, a study assessed the temporal and spatial variations in the leaf area index (LAI) across different vegetation types and their correlations with precipitation and temperature [33]. Furthermore, the total gross primary productivity (GPP) of vegetation in the Poyang Lake basin from 2000 to 2013 was simulated and analyzed, along with its relationships to climatic factors [34]. Another study investigated the temporal and spatial patterns of climatic

variables in the watershed from 1960 to 2020 and examined changes in terrestrial vegetation cover using Enhanced Vegetation Index (EVI) data [35].

However, these studies predominantly focus on historical simulations of micro-level vegetation metrics, such as vegetation cover and vegetation indices, while lacking macro-scale simulations of vegetation type distribution across the region and dynamic projections under future scenarios. To address these challenges, this study integrates High-Accuracy Surface Modeling (HASM) with an improved HLZ model. Using climate observation data from 1961 to 2020 and future scenario projections from the Sixth Coupled Model Intercomparison Project (CMIP6) for the next thirty years under SSP1-2.6, SSP2-4.5, and SSP5-8.5 scenarios, the study explores the spatial relationships between vegetation, climate, and topographical factors in the basin. By establishing classification criteria for vegetation ecosystems, it aims to dynamically simulate vegetation distributions under various scenarios, predict spatiotemporal changes in vegetation patterns, and elucidate the responses of the basin's vegetation ecosystems to climate change.

2. Materials and Methods

2.1. Study Area

The Poyang Lake basin is located on the southern bank of the middle reaches of the Yangtze River (113°35′–118°29′ E, 24°29′–30°05′ N). It encompasses the watersheds of the Gan, Fu, Xin, Rao, and Xiu Rivers, along with the Poyang Lake area, covering approximately 160,000 km^2, 97% of which lies within Jiangxi Province. As one of China's most representative inland basins, its terrain slopes from south to north, descending from the eastern, southern, and western regions toward the Poyang Lake area. The basin features diverse landforms, predominantly mountains (36%) and hills (42%), with ridges, plains, and water bodies comprising the remaining 22%. Situated in a subtropical humid monsoon climate zone, the basin experiences an average annual precipitation of 1662.9 mm and a mean annual temperature of 18.2 °C. It serves as a transitional zone between warm temperate and subtropical vegetation ecosystems, making it a critical ecological conservation area for the middle and lower reaches of the Yangtze River. The region's unique natural geographic conditions support diverse vegetation types with extensive spatial distribution. Consequently, studying the Poyang Lake basin provides valuable insights into how vegetation ecosystems in southern China respond to environmental changes.

The Poyang Lake basin is rich in biodiversity, encompassing a variety of ecosystems, including lake wetlands, farmland, forests, and grasslands. The basin's forest resources and biodiversity are abundant, making it one of the origin centers of the tropical and subtropical flora of Southeast Asia [36,37]. As a major forested region in southern China's subtropical zone, the forest cover remains stable at 63.1%. The majority of the forests are natural secondary forests involving coniferous forests, broadleaf forests, shrubland, and bamboo (Figure 1). Therefore, research in this basin is crucial for better understanding the response of southern China's vegetation ecosystems to ecological and environmental changes.

2.2. Data Collection

The climate data used in this study include both observational records and scenario-based simulation data. Observational data were obtained from daily climate records (1961–2020) collected at 104 meteorological stations within and around the Poyang Lake basin (Figures 1a and 2b). These records include temperature, precipitation, elevation, latitude, longitude, and date information, sourced from the National Climate Center of the China Meteorological Administration. Scenario-based climate data selected in this paper include the three scenarios of SSP1-2.6 (low emissions), SSP2-4.5 (medium emissions), and SSP5-8.5 (high emissions), which were derived from Coupled Model Intercomparison

Project Phase 6 (CMIP6) and downloaded from the website of the World Climate Research Program (https://esgf-node.llnl.gov/projects/cmip6/, accessed on 11 May 2020). These scenarios enabled the simulation of spatiotemporal changes in vegetation ecosystems in the Poyang Lake basin from 2021 to 2050. The geographical location of the study area and the distribution of meteorological stations are depicted in Figure 2. Topographic data for the basin were sourced from the Shuttle Radar Topography Mission (SRTM) database. The original digital elevation model (DEM) data, with a spatial resolution of 90 m × 90 m, were resampled to 250 m × 250 m using the nearest-neighbor method.

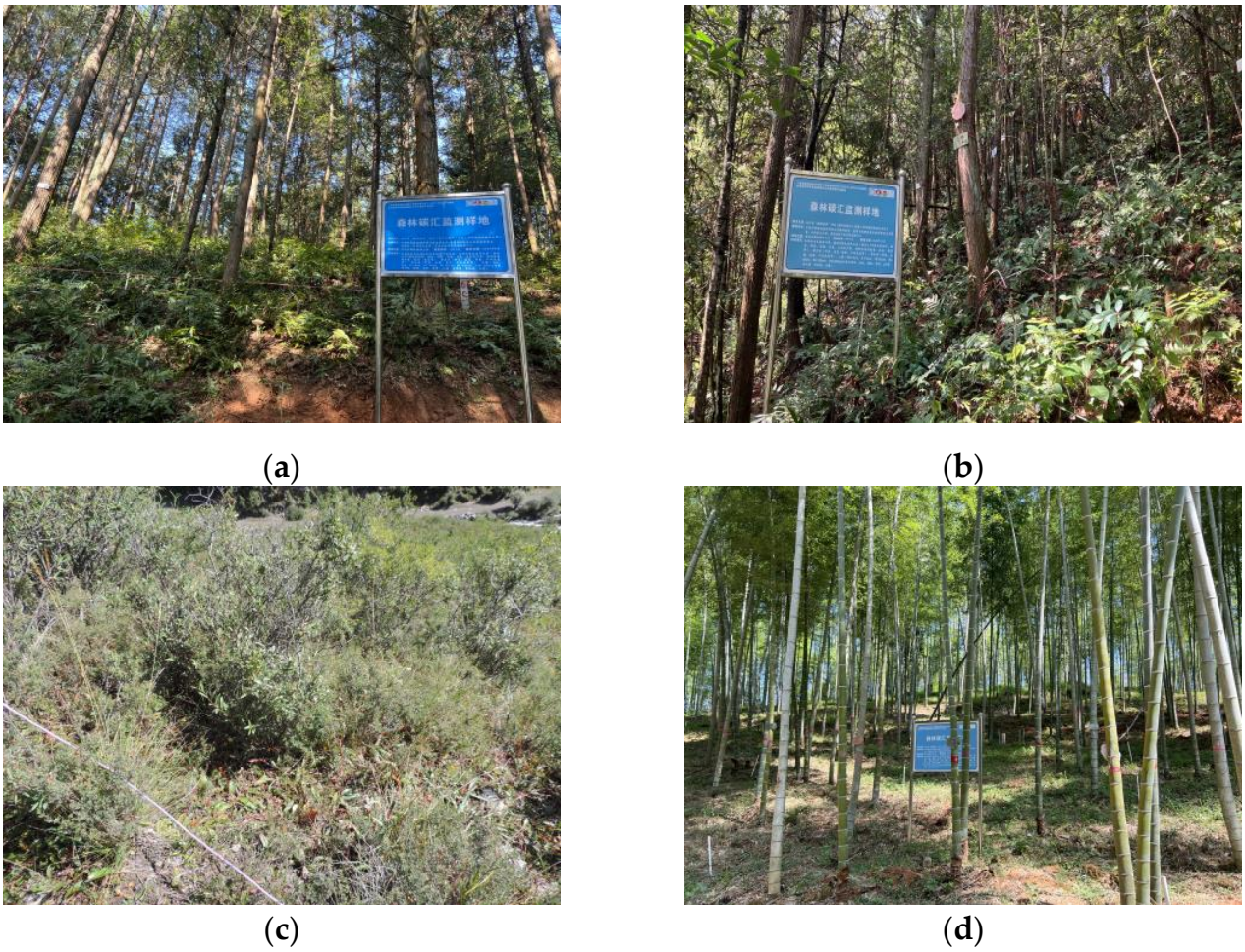


Figure 1. Photographs of the major vegetation types in the Poyang Lake basin. (**a**) Coniferous forests; (**b**) broadleaf forests; (**c**) shrubland; (**d**) bamboo.

Vegetation data were derived from the scanned digital version of the Vegetation Map of China (1:1,000,000 scale). Classification was based on the Revised Scheme of China's Vegetation Classification System [14], incorporating the general distribution of vegetation types in the basin and study objectives. Vegetation types were categorized into 15 classes: temperate grassland, temperate shrubland, temperate marsh, temperate coniferous forest, temperate deciduous broadleaf forest, subtropical grassland, subtropical shrubland, subtropical marsh, subtropical coniferous forest, subtropical deciduous broadleaf forest, subtropical evergreen broadleaf forest, subtropical evergreen–deciduous broadleaf mixed forest, subtropical coniferous–broadleaf mixed forest, bamboo forest, cultivated vegetation, and water bodies (Figure 2c). Auxiliary data from vegetation field surveys in Zixi County, within the Poyang Lake basin, were collected for accuracy verification.

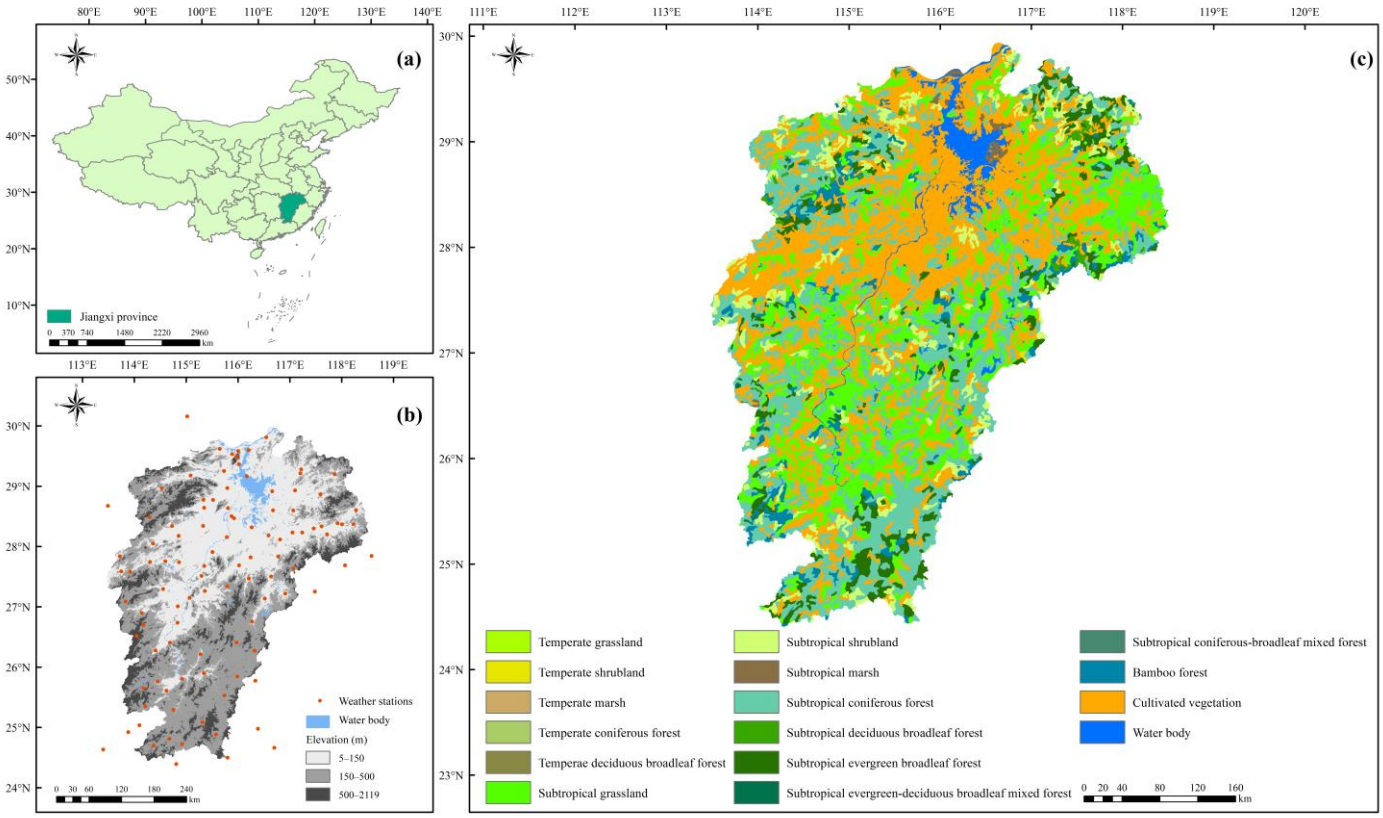


Figure 2. (**a**) Location of study area in China; (**b**) DEM and climate stations in the Poyang Lake basin; (**c**) Vegetation distribution of the Poyang Lake basin in 2010.

2.3. Identification and Simulation Method of Vegetation Distribution

2.3.1. Spatial Interpolation and Downscaling Method of Key Climatic Parameters

The accuracy of spatial interpolation for historical climate observation data and the downscaling of future climate scenario data critically influences the quality of vegetation simulations in the Poyang Lake basin. Methods for spatial interpolation and downscaling include the Inverse Distance Weighting (IDW) model, Triangulated Irregular Network (TIN) model, Kriging model, Spline interpolation model, and the High-Accuracy Surface Modeling (HASM) method [38]. HASM is a new method based on the differential geometry theory that can overcome the drawbacks of the IDW, Kriging, Spline, and TIN interpolation methods, and the accuracy of the interpolated and downscaled climate data is generally improved by approximately 5% compared to that of the other three methods [39,40]. Thus, the HASM method was selected to obtain the spatial grid data of MAB, TAP, and PER at a spatial resolution of 250 m × 250 m by integrating longitude, latitude, and elevation data in the Poyang Lake basin.

The principle can be expressed as follows:

$$Surface = Surf_{trend} + Surf_{residual} \quad (1)$$

where $Surf_{trend}$ represents the trend surface obtained through regression analysis combined with traditional interpolation methods. $Surf_{residual}$ denotes the fitted residual surface interpolated using the HASM method. $Surface$ refers to the high-accuracy surface obtained through spatial interpolation or downscaling.

The historical climate observation data were interpolated from point data into a 250 m spatial resolution surface dataset. The steps for spatial interpolation using the HASM method are as follows: (1) Based on observational data from 104 meteorological stations

in the Poyang Lake basin and its surrounding areas from 1961 to 2020, six time periods were defined at decadal intervals: 1960s, 1970s, 1980s, 1990s, 2000s, and 2010s. The mean annual biotemperature (MAB) and total annual precipitation (TAP) were calculated for each station within these time periods. (2) Using station latitude, longitude, and elevation, the attribute data were transformed into spatial datasets. (3) A multiple linear regression analysis was conducted, using longitude, latitude, and elevation as independent variables for the biological temperature data, and geographically weighted regression (GWR) analysis was performed, using longitude, latitude, slope, aspect, and station elevation as independent variables for precipitation data. Regression equations and residuals were obtained. (4) Biharmonic spline interpolation and the IDW method were used to interpolate the annual mean biological temperature and precipitation point data, generating trend surfaces. (5) The HASM method was applied to interpolate the residuals, generating fitted residual surfaces. (6) The trend surface and residual surface were superimposed to obtain the 250 m × 250 m resolution raster data of climate variables in the Poyang Lake basin from 1961 to 2020.

Future climate scenario data from CMIP6 were downscaled from 1 km to 250 m resolution using the HASM method. The steps for downscaling are as follows: (1) using the climate raster data from 2011 to 2020 as the baseline climate data, the future climate scenario data between 2021 and 2050 were divided into three time periods at decadal intervals: 2020s, 2030s and 2040s; (2) the corresponding CMIP6 data were extracted at the station coordinates to obtain future climate scenario spatial point data; (3) differences between the baseline climate data and CMIP6 point data for the same period were calculated to calibrate the scenario data against the baseline; (4) the difference raster between the CMIP6 data and the calibrated baseline data was calculated, and geographically weighted regression was performed on the difference raster using auxiliary variables such as latitude, longitude, and elevation; (5) the IDW method was used to interpolate the residuals, generating a residual surface; (6) the HASM method was applied to downscale the residual surface; (7) the baseline climate data surface was superimposed with the residual surface to obtain the downscaled raster data for each climate scenario variable from 2021 to 2050. The technical flowchart is shown in Figure 3.

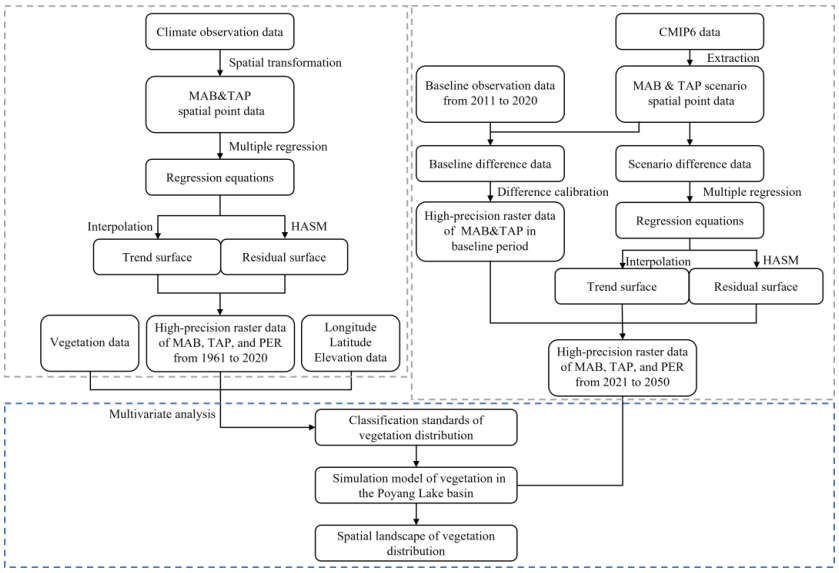


Figure 3. The key technical flowchart of vegetation type classification. The roadmap is divided into three main modules: spatial interpolation of historical climate data (on the left), downscaling of future scenario data (on the right), and construction of the vegetation simulation model (at the bottom).

2.3.2. Classification Standards of Vegetation Distribution

The diverse environmental conditions across the Earth's surface play a fundamental role in shaping the variation in plant community types and their distribution patterns [41]. Vegetation distribution is determined by a combination of environmental factors, including climate, soil, and topography [42]. The HLZ ecosystem model spatially characterizes vegetation types and their potential distributions based on three key bioclimatic variables: mean annual biotemperature (MAB), total annual precipitation (TAP), and the potential evapotranspiration ratio (PER) [43]. Building on the refinement and expansion of the HLZ model's input parameters, this study incorporates six primary bio-environmental factors to classify vegetation types: biotemperature, precipitation, potential evapotranspiration ratio, latitude, longitude, and elevation (Figure 3).

Biotemperature refers to the accumulated temperature during periods when the temperature is above 0 °C but below 30 °C within a given cycle. Evapotranspiration is the total volume of water vapor returning to the atmosphere through evaporation and transpiration. Potential evapotranspiration refers to the amount of water that could potentially evaporate and transpire under optimal soil moisture and vegetation cover conditions. PER, defined as the ratio of mean annual potential evapotranspiration to mean annual precipitation, serves as a key indicator for biological humidity conditions.

The steps for constructing the vegetation classification criteria for the Poyang Lake basin are as follows: (1) convert vegetation attribute data into raster data with a spatial resolution of 250 m; (2) use masking techniques to extract historical climate factor raster data (from 1961 to 2020) and topographic data corresponding to different vegetation types, obtaining sixty-year averaged bio-environmental factor raster data for each vegetation type; (3) conduct multivariate analysis on the bio-environmental factor raster data to develop classification criteria for 15 vegetation types and non-vegetated areas (water bodies) in the Poyang Lake basin. The vegetation types include temperate grassland, temperate shrubland, temperate marsh, temperate coniferous forest, temperate deciduous broadleaf forest, subtropical grassland, subtropical shrubland, subtropical marsh, subtropical coniferous forest, subtropical deciduous broadleaf forest, subtropical evergreen broadleaf forest, subtropical evergreen–deciduous mixed broadleaf forest, subtropical mixed needleleaf–broadleaf forest, bamboo forest, cultivated vegetation, and non-vegetated area (Table 1).

Table 1. The classification criteria of vegetation type in the Poyang Lake basin.

Vegetation	MAB (°C)	TAP (mm)	PER	DEM (m)	LON	LAT
Temperate grassland	16.55	1721.80	0.58	28.82	116.29	29.53
Temperate shrubland	17.15	1860.88	0.55	353.79	115.68	27.25
Temperate marsh	17.25	1788.54	0.57	155.39	117.24	29.71
Temperate coniferous forest	17.74	1804.08	0.58	485.50	116.39	26.25
Temperate deciduous broadleaf forest	17.08	1701.58	0.59	43.75	116.86	29.60
Subtropical grassland	17.98	1790.06	0.60	247.93	115.86	27.42
Subtropical shrubland	17.32	1788.64	0.58	320.81	115.70	27.79
Subtropical marsh	17.55	1666.68	0.64	153.66	116.26	29.09
Subtropical coniferous forest	17.73	1776.20	0.60	313.60	115.51	27.21
Subtropical deciduous broadleaf forest	16.41	2024.78	0.49	414.99	116.54	28.74
Subtropical evergreen broadleaf forest	17.16	1875.00	0.55	435.37	115.94	27.26
Subtropical evergreen–deciduous broadleaf mixed forest	15.51	1900.71	0.48	721.47	113.87	26.75
Subtropical coniferous–broadleaf mixed forest	17.59	1695.86	0.61	295.02	114.10	26.73
Bamboo forest	16.78	1902.48	0.53	474.15	115.53	27.23
Cultivated vegetation	18.18	1724.14	0.63	135.28	115.73	27.96
Water body	18.34	1599.16	0.69	34.76	116.14	28.78

2.3.3. Identification Method of Vegetation Type

The HLZ ecosystem model has been widely used to simulate the potential vegetation pattern on a large scale, which involves three key climate parameters of MAB, TAP, and PER [17,26–29,43]. To further improve the HLZ ecosystem model for simulating the actual vegetation distribution, the number of input parameters were increased from three to six, including MAB, TAP, PER, longitude (LON), latitude (LAT), and elevation (DEM). This approach establishes a spatial simulation model for vegetation ecosystem distribution within the basin. By integrating the vegetation type classification criteria for the Poyang Lake basin and the formulae in the HLZ ecosystem model [43], the theoretical computational formula for identifying the actual vegetation distribution is expressed as follows:

$$M(x,y,t) = \log_2 MAB(x,y,t) = \log_2\left[\frac{1}{365}\sum_{j=1}^{365} Tem_{>0}(j,x,y,t)\right] \quad (2)$$

$$T(x,y,t) = \log_2 TAP(x,y,t) = \log_2 \sum_{j=1}^{365} P(j,x,y,t) \quad (3)$$

$$P(x,y,t) = \log_2 PER(x,y,t) = \log_2 \frac{58.93MAB(x,y,t)}{TAP(x,y,t)} \quad (4)$$

$$L(x,y,t) = \log_2 LON(x,y,t) \quad (5)$$

$$B(x,y,t) = \log_2 LAT(x,y,t) \quad (6)$$

$$D(x,y,t) = \log_2 DEM(x,y,t) \quad (7)$$

$$HLZ_i(x,y,t) = \sqrt{\begin{array}{c}(M(x,y,t)-M_{i_0})^2+(T(x,y,t)-T_{i_0})^2+(P(x,y,t)-P_{i_0})^2+\\ (L(x,y,t)-L_{i_0})^2+(B(x,y,t)-B_{i_0})^2+(D(x,y,t)-D_{i_0})^2\end{array}} \quad (8)$$

where $MAB(x,y,t)$, $TAP(x,y,t)$, $PER(x,y,t)$ represent mean annual biotemperature (°C), total annual precipitation (mm), and potential evapotranspiration ratio at location (x,y) at time t, respectively. $Tem_{>0}(j,x,y,t)$ denotes the accumulated biotemperature on the j-th day exceeding 0 °C, while $P(j,x,y,t)$ represents the average precipitation on the same day. $LON(x,y,t)$, $LAT(x,y,t)$, $DEM(x,y,t)$ denote the longitude, latitude, and elevation of location at location (x,y) at time t, respectively. M_{i_0}, T_{i_0}, P_{i_0}, L_{i_0}, B_{i_0}, D_{i_0} are the logarithmic standard reference values for the mean temperature, precipitation, potential evapotranspiration ratio, longitude, latitude, and elevation of vegetation type i in the Poyang Lake basin. $HLZ_i(x,y,t)$ is the vegetation type at location (x,y) at time t. When $HLZ_k(x,y,t) = min\{HLZ_i(x,y,t)\}$, the point (x,y) is classified as vegetation type k.

3. Results

3.1. Accuracy Verification

The accuracy of vegetation type simulations under current biophysical conditions was evaluated using field survey data. Since up-to-date vegetation data for the entire Poyang Lake basin were unavailable, field observations collected in 2020 from Zixi County, Jiangxi Province, were used as reference data. These surveys provided detailed information on vegetation communities within the county.

Following established vegetation classification principles, the field data were systematically processed, and accuracy assessments were conducted using a confusion matrix (Table 2), overall accuracy, and the Kappa coefficient. Zixi County contains nine major vegetation types: temperate coniferous forest, temperate deciduous broadleaf forest, subtropical coniferous forest, subtropical deciduous broadleaf forest, subtropical evergreen broadleaf forest, subtropical evergreen–deciduous broadleaf mixed forest, subtropical coniferous–broadleaf mixed forest, bamboo forest, and cultivated vegetation. Overall classification

accuracy is defined as the proportion of correctly classified pixels for a given vegetation type relative to the total number of pixels. The Kappa coefficient, derived from the confusion matrix, quantifies the level of agreement between the model's simulation results and the actual vegetation distribution. Results from the confusion matrix indicate an overall accuracy of 79.60%, with a Kappa coefficient of 0.76, suggesting a strong correlation between the simulated vegetation map and the field survey data. These findings confirm that the proposed methodology is effective for simulating spatiotemporal changes in vegetation types across the Poyang Lake basin under future climate scenarios.

Table 2. Confusion matrix of true values and predicted values of vegetation types in Zixi County.

Predicted Values											
0	0	0	0	0	0	0	0	0	0	0	0
0	1	0	0	0	0	0	0	0	0	0	0
26	0	210	73	4	0	0	0	0	0	0	0
0	0	0	0	0	0	0	0	0	0	0	0
0	0	0	0	0	0	0	0	0	0	0	0
810	0	0	1746	47	3485	114	0	0	0	0	0
2	0	0	0	1	0	3718	0	0	0	0	0
350	0	0	520	32	0	17	5327	4	0	0	0
114	0	0	143	4	0	10	0	1388	0	0	0
42	0	0	80	4	0	4	0	0	231	0	0
704	0	0	854	42	0	17	0	0	0	4746	0
0	0	0	0	0	0	0	0	0	0	0	3382

3.2. Spatial Landscape of Vegetation Distribution

Using climate observation data MAB and TAP (Figure 4a,b) from 2011 to 2020 and the simulation model, the simulated spatial landscape of vegetation distribution in 2020 was obtained, which is shown in Figure 1c. The results in Figure 1d show that cultivated vegetation would occupy the largest area, accounting for 34.93% of the total, primarily distributed around the northern Poyang Lake region and the central plains. In addition to cultivated vegetation, subtropical coniferous forest, subtropical grassland, and subtropical shrub would be the main natural vegetation types in the Poyang Lake basin, covering 21.59%, 19.36%, and 5.10% of the total area, respectively. Subtropical coniferous forest is mainly distributed in the hilly and mountainous areas of the south-central region, subtropical grassland would primarily be found in the hilly areas of the south-central region, and subtropical shrubland would be scattered across the higher-elevation areas of the entire basin (Figure 4d).

3.3. Dynamic Changes in Vegetation Area

Statistical analysis of the simulated vegetation types in the Poyang Lake basin under the SSP1-2.6, SSP2-4.5, and SSP5-8.5 scenarios (Figure 5) indicates that the total number of vegetation types would remain unchanged over the next 30 years. Fifteen vegetation types—including temperate grassland, temperate shrubland, temperate marsh, temperate coniferous forest, temperate deciduous broadleaf forest, subtropical grassland, subtropical shrubland, subtropical marsh, subtropical coniferous forest, subtropical deciduous broadleaf forest, subtropical evergreen broadleaf forest, subtropical evergreen–deciduous broadleaf mixed forest, subtropical coniferous–broadleaf mixed forest, bamboo forest, and cultivated vegetation—would persist across all time periods under the three scenarios. However, their spatial distribution and extent would exhibit distinct trends and spatial variations.

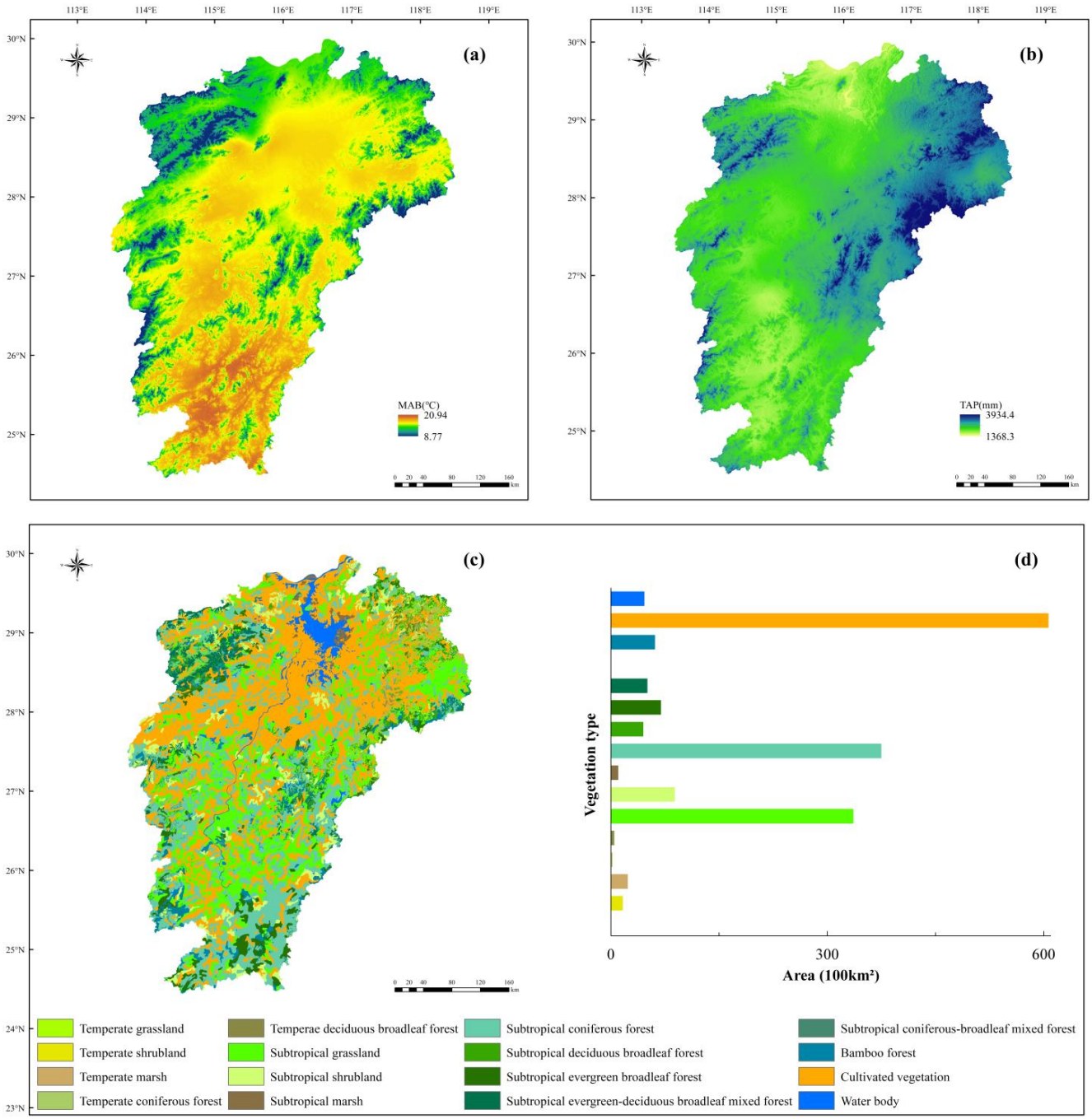


Figure 4. (**a**–**c**) Spatial distribution of MAB, TAP, and simulated vegetation in the Poyang Lake basin in 2020; (**d**) areas of simulated vegetation in 2020.

Under the SSP1-2.6 scenario (Figure 6a, Table 3), subtropical coniferous forest, subtropical grassland, and temperate marsh would experience the greatest reductions, decreasing by an average of 29.92 × 10^2 km^2, 11.70 × 10^2 km^2, and 5.41 × 10^2 km^2, respectively. Conversely, subtropical evergreen–deciduous broadleaf mixed forest, bamboo forest, and temperate shrubland would exhibit the largest expansions, increasing by 19.05 × 10^2 km^2, 9.41 × 10^2 km^2, and 8.27 × 10^2 km^2 per decade, respectively. Additionally, the area of temperate marsh would decline by 69%, whereas temperate grassland, temperate coniferous forest, subtropical marsh, and subtropical coniferous–broadleaf mixed forest would increase by more than 150%. These findings suggest that these vegetation types are particularly sensitive to climate change.

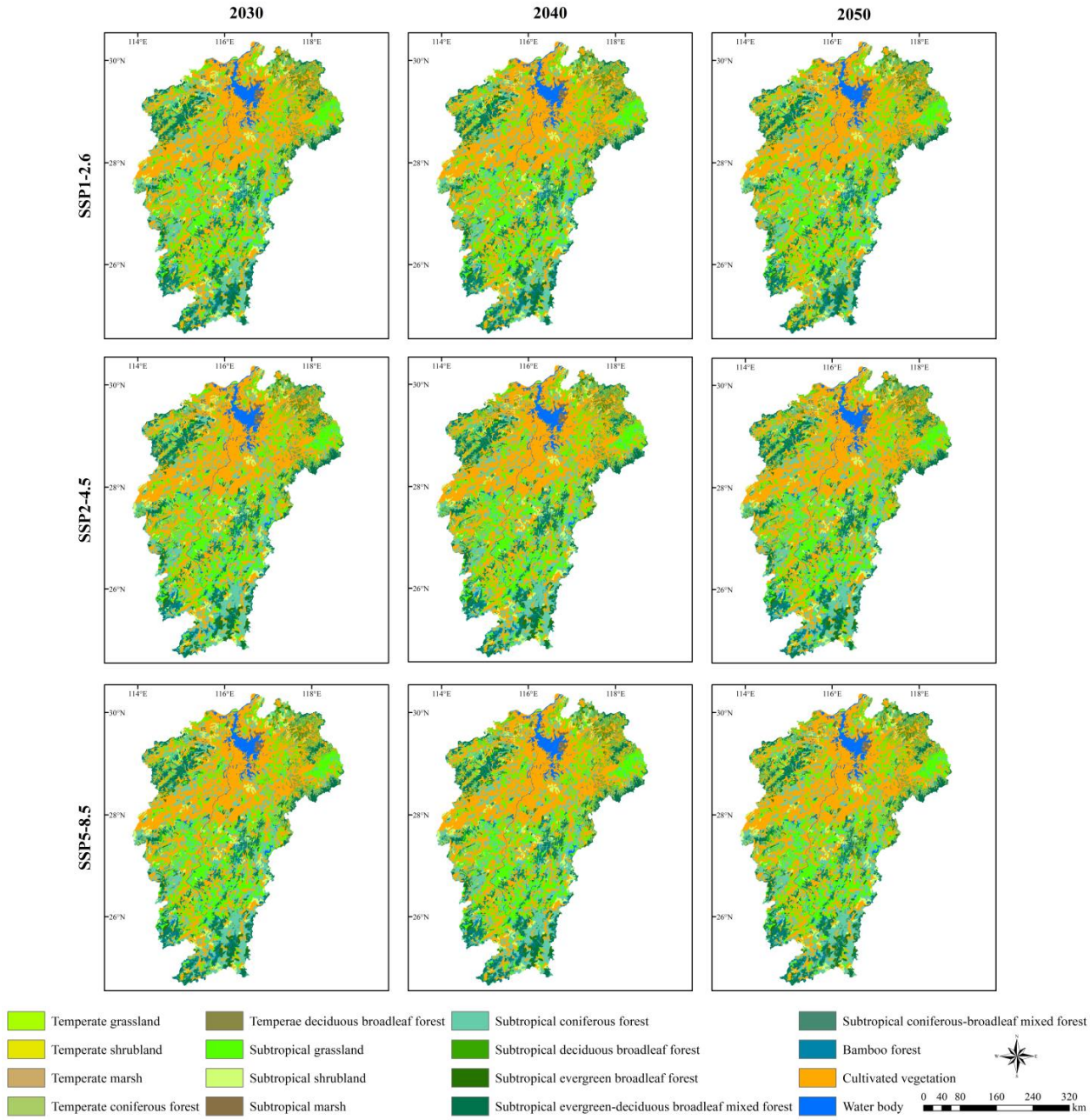


Figure 5. Spatiotemporal distributions of vegetation under climate change scenarios (SSP1-2.6, SSP2-4.5, and SSP5-8.5) in 2030, 2040, and 2050.

Table 3. Changes in the area (100 km^2) of vegetation in the Poyang Lake basin under SSP1-2.6 from 2020 to 2050.

Vegetation	2020	2030	2040	2050
Temperate grassland	1.82	1.37	1.37	1.37
Temperate shrubland	16.63	22.92	25.42	27.85
Temperate marsh	23.40	7.32	7.15	7.11
Temperate coniferous forest	2.26	17.30	19.32	35.92
Temperate deciduous broadleaf forest	4.57	4.90	4.89	4.89
Subtropical grassland	336.23	306.73	307.25	303.11
Subtropical shrubland	88.53	87.39	86.64	84.59
Subtropical marsh	10.18	24.47	26.29	26.20
Subtropical coniferous forest	375.01	314.03	305.78	299.43

Table 3. *Cont.*

Vegetation	2020	2030	2040	2050
Subtropical deciduous broadleaf forest	44.98	16.25	14.67	7.20
Subtropical evergreen broadleaf forest	69.53	63.13	64.21	72.32
Subtropical evergreen–deciduous broadleaf mixed forest	50.66	107.89	109.78	111.70
Subtropical coniferous–broadleaf mixed forest	0.44	18.26	20.69	24.71
Bamboo forest	61.16	85.56	84.07	71.10
Cultivated vegetation	606.55	611.68	611.70	611.72
Water body	-	-	-	-

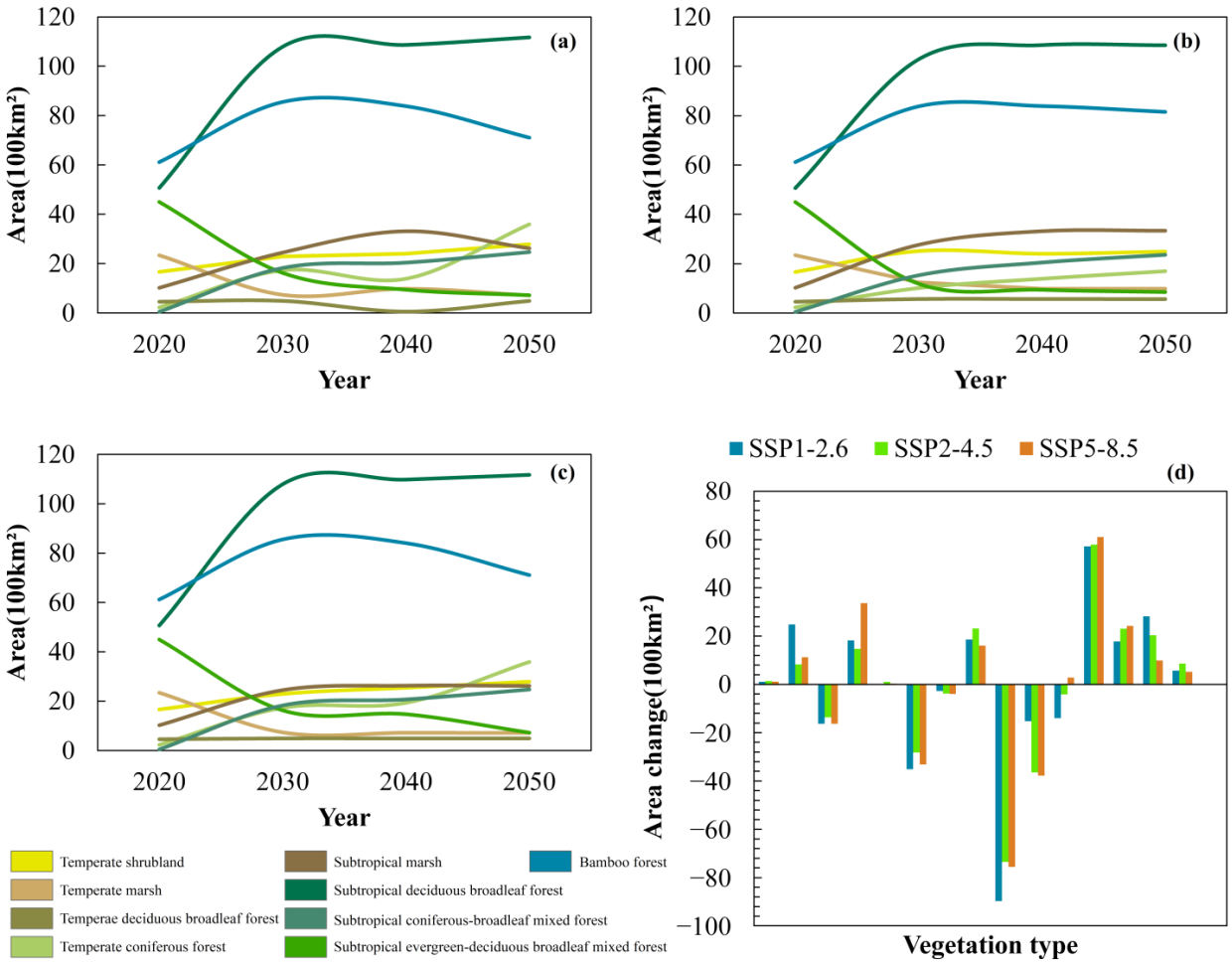


Figure 6. Area of vegetation with significant changes across different years under (**a**) SSP1-2.6, (**b**) SSP2-4.5, and (**c**) SSP5-8.5; (**d**) The differences in area changes under climate change scenarios.

Under the SSP2-4.5 scenario (Figure 6b, Table 4), subtropical coniferous forest, subtropical deciduous broadleaf forest, and subtropical grassland would undergo the most significant reductions, decreasing by 24.51 × 10^2 km^2, 12.15 × 10^2 km^2, and 9.39 × 10^2 km^2 per decade, respectively. In contrast, subtropical evergreen–deciduous broadleaf mixed forest, subtropical marsh, and subtropical coniferous–broadleaf mixed forest would exhibit the highest growth, expanding by 19.30 × 10^2 km^2, 7.71 × 10^2 km^2, and 7.70 × 10^2 km^2, respectively. Compared to 2020, the subtropical deciduous broadleaf forest area would decline by 81%, while the areas of temperate grassland, temperate coniferous forest, subtropical marsh, and subtropical coniferous–broadleaf mixed forest all would increase by more than 200%. These results suggest that vegetation types such as temperate grassland,

temperate coniferous forest, subtropical marsh, subtropical deciduous broadleaf forest, and subtropical coniferous–broadleaf mixed forest are particularly sensitive to climate change.

Under the SSP5-8.5 scenario (Figure 6c, Table 5), subtropical coniferous forest, subtropical deciduous broadleaf forest, and subtropical grassland would show the largest reductions, with an average decadal decrease of 25.20 $\times$ 10^2 km^2, 12.59 $\times$ 10^2 km^2, and 11.04 $\times$ 10^2 km^2, respectively. Meanwhile, temperate coniferous forest, subtropical evergreen–deciduous broadleaf mixed forest, and subtropical coniferous–broadleaf mixed forest would undergo the most substantial expansions, increasing by 20.35 $\times$ 10^2 km^2, 11.22 $\times$ 10^2 km^2, and 8.09 $\times$ 10^2 km^2 per decade, respectively. Additionally, the subtropical deciduous broadleaf forest area would decline by 84%, while temperate marsh would shrink by nearly 70%. The areas of temperate grassland, temperate coniferous forest, subtropical marsh, and subtropical coniferous–broadleaf mixed forest would increase by more than 155%, further highlighting their sensitivity to climate change.

Table 4. Changes in the area (100 km^2) of vegetation in the Poyang Lake basin under SSP2-4.5 from 2020 to 2050.

Vegetation	2020	2030	2040	2050
Temperate grassland	1.82	1.62	1.62	1.62
Temperate shrubland	16.63	25.12	24.03	24.91
Temperate marsh	23.40	12.43	9.81	9.80
Temperate coniferous forest	2.26	10.11	13.88	16.96
Temperate deciduous broadleaf forest	4.57	5.64	5.63	5.62
Subtropical grassland	336.23	310.55	307.68	308.06
Subtropical shrubland	88.53	87.30	85.59	84.77
Subtropical marsh	10.18	27.60	33.12	33.31
Subtropical coniferous forest	375.01	315.34	306.02	301.48
Subtropical deciduous broadleaf forest	44.98	11.88	9.43	8.52
Subtropical evergreen broadleaf forest	69.53	65.81	64.34	65.41
Subtropical evergreen–deciduous broadleaf mixed forest	50.66	102.87	108.64	108.57
Subtropical coniferous–broadleaf mixed forest	0.44	15.26	20.42	23.54
Bamboo forest	61.16	83.74	83.86	81.49
Cultivated vegetation	606.55	614.96	615.14	615.15
Water body	-	-	-	-

Table 5. Changes in the area (100 km^2) of vegetation in the Poyang Lake basin under SSP5-8.5 from 2020 to 2050.

Vegetation	2020	2030	2040	2050
Temperate grassland	1.82	1.37	1.37	1.37
Temperate shrubland	16.63	22.92	25.42	27.85
Temperate marsh	23.40	7.32	7.15	7.11
Temperate coniferous forest	2.26	17.30	19.32	35.92
Temperate deciduous broadleaf forest	4.57	4.90	4.89	4.89
Subtropical grassland	336.23	306.73	307.25	303.11
Subtropical shrubland	88.53	87.39	86.64	84.59
Subtropical marsh	10.18	24.47	26.29	26.20
Subtropical coniferous forest	375.01	314.03	305.78	299.43
Subtropical deciduous broadleaf forest	44.98	16.25	14.67	7.20
Subtropical evergreen broadleaf forest	69.53	63.13	64.21	72.32
Subtropical evergreen–deciduous broadleaf mixed forest	50.66	107.89	109.78	111.70
Subtropical coniferous–broadleaf mixed forest	0.44	18.26	20.69	24.71
Bamboo forest	61.16	85.56	84.07	71.10
Cultivated vegetation	606.55	611.68	611.70	611.72
Water body	-	-	-	-

In summary, combining the dynamic changes in vegetation areas across the three scenarios (Figure 6d), temperate grassland, temperate coniferous forest, temperate/subtropical marsh, subtropical deciduous broadleaf forest, and subtropical coniferous–broadleaf mixed forest would exhibit the greatest sensitivity to climate change compared to other vegetation types.

3.4. Change Intensity of Vegetation

To better analyze the characteristics of vegetation changes in the Poyang Lake basin under different climate scenarios, the region's terrain was categorized into three elevation gradients: low (<150 m), medium (150–500 m), and high (>500 m) [44,45]. Using the vegetation distribution simulation results under SSP1-2.6, SSP2-4.5, and SSP5-8.5, spatial statistical and comparative analyses are conducted to assess vegetation changes across different elevations. The findings (Tables 6–8) reveal that the intensity of vegetation type changes would be greatest under the SSP5-8.5 scenario, followed by SSP1-2.6, with SSP2-4.5 exhibiting the least change. Between 2021 and 2030, the Poyang Lake basin would experience the most intense vegetation type changes, with the affected area accounting for 64.6%, 56.32%, and 62.17% of the total area under the three scenarios, respectively. From 2030 to 2040, vegetation would change slow significantly under the SSP1-2.6 and SSP5-8.5 scenarios, with the affected area comprising only 4.27% and 5.19%, respectively. In contrast, under SSP2-4.5, the least vegetation change would occur between 2041 and 2050, with the affected area making up just 3.5% of the total.

Table 6. The intensity (%) of vegetation changes in different elevation zones under the SSP1-2.6 scenario.

Area	2021–2030	2031–2040	2041–2050
Low-elevation area	1.36	0.042	0.003
Medium-elevation area	20.34	2.49	3.99
High-elevation area	42.90	1.74	1.41
The whole region	64.60	4.27	5.40

Table 7. The intensity (%) of vegetation changes in different elevation zones under the SSP2-4.5 scenario.

Area	2021–2030	2031–2040	2041–2050
Low-elevation area	1.98	0.092	0
Medium-elevation area	17.27	3.65	1.871
High-elevation area	37.07	4.82	1.626
The whole region	56.32	8.57	3.50

Table 8. The intensity (%) of vegetation changes in different elevation zones under the SSP5-8.5 scenario.

Area	2021–2030	2031–2040	2041–2050
Low-elevation area	1.26	0.006	0.004
Medium-elevation area	18.07	2.85	4.39
High-elevation area	42.841	2.33	7.50
The whole region	62.17	5.19	11.89

Across all three scenarios, vegetation changes would be most pronounced in high-altitude regions, while low-altitude areas would exhibit the slowest shifts. Over the next three decades, the proportion of vegetation change in high-altitude areas would account for 45.50%, 42.19%, and 49.63% of the total high-altitude area under the three scenarios, respectively. Conversely, vegetation change in low-altitude areas would remain minimal, at 1.40%, 2.06%, and 1.26%, respectively. Overall, from 2021 to 2050, the intensity of vegetation type changes in the Poyang Lake basin would show a clear increasing trend with elevation under all three climate change scenarios.

4. Discussion

This study examines the spatiotemporal dynamics of vegetation types within the Poyang Lake basin, focusing on fine-scale simulations of their temporal evolution, spatial distribution, and patterns by integrating climatic and topographic factors. In vegetation ecosystem modeling, the HLZ model is a well-established tool for simulating the spatial distribution of vegetation ecosystems [26,46–48]. This model quantitatively characterizes vegetation types and their potential distributions based on climatic parameters over medium- to long-term timescales. The improved HLZ model has been widely applied to large-scale simulations of potential vegetation dynamics, ecotone delineation, land cover change projections, and ecological zoning [29,43,49,50].

However, previous studies have primarily focused on ecosystem evolution at coarse spatial resolutions, spanning extensive spatiotemporal scales, thereby lacking the precision required for fine-scale identification and habitat modeling of diverse vegetation ecosystems within specific regions. To address this limitation, the present study integrates actual vegetation data and topographic features of the Poyang Lake basin into the improved HLZ model to quantitatively simulate and analyze vegetation types and their spatial patterns within the basin. Validation against existing vegetation datasets demonstrates high accuracy, enabling reliable scenario-based projections of vegetation spatial dynamics.

The vegetation dynamics of the Poyang Lake basin are shaped by its unique environmental conditions [51]. Interannual fluctuations in water levels along the lake's shores foster the development of floodplain and marsh vegetation, aligning with the distribution of subtropical marsh ecosystems identified in this study. Coniferous forests dominate the hilly areas below 1000 m, while evergreen–deciduous broadleaf mixed forests are characteristic of the northern subtropical region [35]. Cultivated vegetation, strongly influenced by human activities, is primarily distributed in plains and hilly terrains surrounding Poyang Lake [52]—a pattern accurately captured in the simulation results.

Under future climate change scenarios, the simulation results indicate that over the next 30 years, substantial shifts will occur in subtropical grassland, temperate and subtropical coniferous forest, subtropical deciduous broadleaf forest, subtropical evergreen–deciduous broadleaf mixed forest, and subtropical coniferous–broadleaf mixed forest. These findings suggest that these vegetation types will be highly responsive to climate change, with coniferous forests exhibiting particularly pronounced sensitivity, corroborating observations by Wu et al. [53]. Moreover, high-elevation vegetation types, such as temperate coniferous forest, subtropical evergreen broadleaf forest, subtropical evergreen–deciduous broadleaf mixed forest, and bamboo forest, will display greater variability across all scenarios compared to mid- and low-elevation vegetation types. This pattern highlights zonal differentiation in vegetation evolution, attributed by Xia to the influence of topographic factors on regional moisture, heat distribution, and land use, which in turn affect vegetation succession [45]. Precipitation within the Poyang Lake basin exhibits a positive correlation with elevation. Higher elevations, characterized by limited human interference, provide favorable hydrothermal conditions and stable environments for vegetation growth, leading to greater vegetation fluctuations in these areas. This suggests that temperature exerts a stronger influence on overall vegetation growth in the basin than precipitation [54]. Furthermore, topographic gradients—particularly slope and elevation—play a crucial role in vegetation transitions [55].

Future complex environmental changes will directly and indirectly influence the structure, function, and succession processes of vegetation ecosystems, through both climate change and human activities [56]. Human activities, including economic development and policy frameworks, significantly contribute to vegetation changes [57]. On one hand, such activities can promote the growth of specific vegetation types, such as through reforesta-

tion and ecological engineering projects [58]. Under the policy-driven SSP1-2.5 scenario, the spatial distribution of vegetation in the Poyang Lake basin is characterized by a shift from monoculture forests to temperate artificial forests and subtropical mixed forests, thus enhancing forest diversity. On the other hand, human activities can also disrupt vegetation growth, as seen in urbanization and agricultural practices [59]. Under the SSP2-4.5 and SSP5-8.5 scenarios, vegetation may be significantly affected by land use changes, leading to a sharp decline in coniferous forests. Future research should focus on the protection of wetland vegetation and marshes surrounding the Poyang Lake basin, alongside the management of vegetation types that are more sensitive to habitat alterations, such as coniferous forests and subtropical evergreen broadleaf mixed forests. This approach would effectively strengthen vegetation resilience to climate change. Changes in vegetation spatial patterns may reflect either environmental degradation or natural adaptation. For example, a reduction in marshes is likely indicative of environmental degradation, which could result in the loss of migratory bird habitats, water quality deterioration, and decreased flood regulation capacity, ultimately increasing the vulnerability of wetland ecosystems and diminishing their ecological functions [60]. Conversely, the projected decrease in subtropical evergreen broadleaf forest from 2020 to 2030, followed by a recovery post-2030, even surpassing their original extent, suggests that vegetation is continuously adjusting and adapting in response to climate change.

5. Conclusions

This study integrates the HASM method with the improved HLZ ecosystem model to incorporate regional climatic and topographic features. It evaluates the spatial distribution and future scenarios of vegetation in the Poyang Lake basin under SSP1-2.6, SSP2-4.5, and SSP5-8.5 climate scenarios from 2021 to 2050, based on CMIP6 data. The analysis finds that cultivated vegetation, subtropical coniferous forest, and subtropical grassland are the most prevalent types, accounting for 34.93%, 21.59%, and 19.36% of the total area, respectively. Among the three scenarios, vegetation type changes are most pronounced under SSP5-8.5 and least under SSP2-4.5. This indicates that the intensity of climate change directly influences the pace of vegetation transformation in the Poyang Lake basin, with the magnitude of future warming emerging as a key driver of vegetation spatial shifts. Temperate and subtropical coniferous forest, subtropical grassland, subtropical deciduous broadleaf forest, and subtropical evergreen–deciduous broadleaf mixed forest in the Poyang Lake basin exhibit greater sensitivity to climate change compared to other types. Furthermore, the intensity of vegetation change is positively correlated with elevation, with high-altitude regions experiencing the most rapid shifts, followed by mid-altitude areas, while low-altitude regions exhibit the least variation, which suggests that vegetation responses to climate change become more pronounced at higher elevations. Consequently, high-altitude ecosystems are particularly vulnerable to climate change, necessitating targeted conservation efforts to mitigate its ecological impacts.

There are still some limitations in current vegetation modeling studies, and future research can be improved and expanded in the following two aspects: (1) Incorporating anthropogenic input parameters: Vegetation spatial distribution patterns are influenced by a variety of factors. Currently, the models only account for climate factors—such as mean bio-temperature, mean annual precipitation, and potential evapotranspiration ratio—and topographic factors, such as elevation and geographical coordinates. Future work should integrate anthropogenic parameters, including population density and transportation accessibility, into the models. This would enhance the accuracy of simulations involving artificial vegetation. (2) Considering the weight of environmental factors. Vegetation types respond differently to changes in environmental factors, yet current research only

considers the average mathematical impact of each factor on vegetation. Future studies could incorporate machine learning and other artificial intelligence techniques to train models using samples of various vegetation types and environmental parameters. This would allow for a more nuanced understanding of the weight relationships between environmental factors and vegetation distribution, ultimately optimizing the simulation of diverse vegetation.

Author Contributions: Conceptualization, Z.F. and L.W.; methodology, L.W. and Z.F.; software, L.W. and S.L.; validation, L.W., Z.F. and Z.D.; formal analysis, L.W. and Z.F.; investigation, L.W. and Z.D.; resources, Z.F., L.W., Y.Y., Z.D. and X.B.; data curation, L.W., Z.F. and Z.D.; writing—original draft preparation, L.W. and Z.F.; writing—review and editing, Z.F. and L.W.; visualization, L.W. and Z.F.; supervision, Z.F.; project administration, Z.F.; funding acquisition, Z.F. All authors have read and agreed to the published version of the manuscript.

Funding: This work was supported by the National Natural Science Foundation of China (Grant Nos. 42293271, 42330707, 41971358, 41930647, and 41931293), and the Innovation Project of State Key Laboratory of Resources and Environmental Information System (KPI005).

Data Availability Statement: The data supporting the findings of this study are available from the following publicly accessible sources: climate data from the CMIP6 project can be found at the IPCC website (https://www.ipcc-data.org/ accessed on 11 February 2025); topographic data were sourced from the Shuttle Radar Topography Mission (SRTM) database (https://srtm.csi.cgiar.org/ accessed on 11 February 2025).

Conflicts of Interest: The authors declare no conflicts of interest.

References

1. Lenoir, J.; Svenning, J.-C. Climate-related Range Shifts—A Global Multidimensional Synthesis and New Research Directions. *Ecography* **2015**, *38*, 15–28. [CrossRef]
2. Bastien-Olvera, B.A.; Conte, M.N.; Dong, X.; Briceno, T.; Batker, D.; Emmerling, J.; Tavoni, M.; Granella, F.; Moore, F.C. Unequal Climate Impacts on Global Values of Natural Capital. *Nature* **2024**, *625*, 722–727. [CrossRef]
3. Otto-Portner, H.; Scholes, B.; Agard, J.; Archer, E.R.M.; Arneth, A.; Bai, X.; Barnes, D.K.A.; Burrows, M.T.; Chan, L.; Cheung, W.L.; et al. *Scientific Outcome of the IPBES-IPCC Co-Sponsored Workshop on Biodiversity and Climate Change*; IPBES Sectetariat: Bonn, Germany, 2021.
4. Pecl, G.T.; Araújo, M.B.; Bell, J.D.; Blanchard, J.; Bonebrake, T.C.; Chen, I.-C.; Clark, T.D.; Colwell, R.K.; Danielsen, F.; Evengård, B.; et al. Biodiversity Redistribution under Climate Change: Impacts on Ecosystems and Human Well-Being. *Science* **2017**, *355*, eaai9214. [CrossRef]
5. Heijmans, M.M.P.D.; Magnússon, R.Í.; Lara, M.J.; Frost, G.V.; Myers-Smith, I.H.; Van Huissteden, J.; Jorgenson, M.T.; Fedorov, A.N.; Epstein, H.E.; Lawrence, D.M.; et al. Tundra Vegetation Change and Impacts on Permafrost. *Nat. Rev. Earth Environ.* **2022**, *3*, 68–84. [CrossRef]
6. Zeng, Y.L.; Hao, D.L.; Huete, A.; Dechant, B.; Berry, J.; Chen, J.M.; Joiner, J.; Frankenberg, C.; Bond-Lamberty, B.; Ryu, Y.; et al. Optical Vegetation Indices for Monitoring Terrestrial Ecosystems Globally. *Nat. Rev. Earth Environ.* **2022**, *3*, 477–493. [CrossRef]
7. Jia, B.Q. Driving factor analysis on the vegetation changes derived from the Landsat TM images in Beijing. *Acta Ecol. Sin.* **2013**, *33*, 1654–1666. [CrossRef]
8. Pitman, A.J. The Evolution of, and Revolution in, Land Surface Schemes Designed for Climate Models. *Int. J. Climatol.* **2003**, *23*, 479–510. [CrossRef]
9. Fan, Z.M.; Fan, B.; Yue, T.X. Terrestrial ecosystem scenarios and their response to climate change in Eurasia. *Sci. China Earth Sci.* **2019**, *49*, 1817–1830. [CrossRef]
10. Bakkenes, M.; Alkemade, J.R.M.; Ihle, F.; Leemans, R.; Latour, J.B. Assessing Effects of Forecasted Climate Change on the Diversity and Distribution of European Higher Plants for 2050. *Glob. Change Biol.* **2002**, *8*, 390–407. [CrossRef]
11. Thomas, C.D.; Cameron, A.; Green, R.E.; Bakkenes, M.; Beaumont, L.J.; Collingham, Y.C.; Erasmus, B.F.N.; de Siqueira, M.F.; Grainger, A.; Hannah, L.; et al. Extinction Risk from Climate Change. *Nature* **2004**, *427*, 145–148. [CrossRef] [PubMed]
12. Qian, S.; Fu, Y.; Pan, F.F. Climate change tendency and grassland vegetation response during the growth season in Three-River Source Region. *Sci. China Earth Sci.* **2010**, *53*, 1506–1512. [CrossRef]
13. Fang, X.Q.; Chen, F.H. Plant phenology and climate change. *Sci. China Earth Sci.* **2015**, *58*, 1043–1044. [CrossRef]

14. Guo, K.; Fang, J.Y.; Wang, G.H.; Tang, Z.Y.; Xie, Z.Q.; Shen, Z.H.; Wang, R.Q.; Qiang, S.; Liang, C.Z.; Da, L.J.; et al. A revised scheme of vegetation classification system of China. *Chin. J. Plant Ecol.* **2020**, *44*, 111–127. [CrossRef]
15. Yue, T.X.; Fan, Z.M. A review of responses of typical terrestrial ecosystems to climate change. *Chin. Sci. Bull.* **2014**, *59*, 217–231. [CrossRef]
16. Li, S.Q.; Zhang, X.; Lu, Z.Y.; Ni, J.; Lu, J.H. Progress of Vegetation Modelling and Future Research Prospects. *Sci. China Earth Sci.* **2024**, *67*, 2718–2738. [CrossRef]
17. Holdridge, L.R. *Life Zone Ecology*; Tropical Science Center: San José, Costa Rica, 1967.
18. Box, E.O. Predicting Physiognomic Vegetation Types with Climate Variables. *Vegetatio* **1981**, *45*, 127–139. [CrossRef]
19. Woodward, F.I.; Williams, B.G. Climate and Plant Distribution at Global and Local Scales. *Vegetatio* **1987**, *69*, 189–197. [CrossRef]
20. Neilson, R.P.; King, G.A.; Koerper, G. Toward a Rule-Based Biome Model. *Landsc. Ecol.* **1992**, *7*, 27–43. [CrossRef]
21. Prentice, I.C.; Cramer, W.; Harrison, S.P.; Leemans, R.; Monserud, R.A.; Solomon, A.M. Special Paper: A Global Biome Model Based on Plant Physiology and Dominance, Soil Properties and Climate. *J. Biogeogr.* **1992**, *19*, 117. [CrossRef]
22. Haxeltine, A.; Prentice, I.C. BIOME3: An Equilibrium Terrestrial Biosphere Model Based on Ecophysiological Constraints, Resource Availability, and Competition among Plant Functional Types. *Glob. Biogeochem. Cycle* **1996**, *10*, 693–709. [CrossRef]
23. Kaplan, J.O. Geophysical Applications of Vegetation Modeling. Ph.D. Thesis, Lund University, Lund, Sweden, 2001.
24. Herzschuh, U.; Ni, J.; Birks, H.J.B.; Böhner, J. Driving Forces of Mid-Holocene Vegetation Shifts on the Upper Tibetan Plateau, with Emphasis on Changes in Atmospheric CO2 Concentrations. *Quat. Sci. Rev.* **2011**, *30*, 1907–1917. [CrossRef]
25. Foley, J.A.; Prentice, I.C.; Ramankutty, N.; Levis, S.; Pollard, D.; Sitch, S.; Haxeltine, A. An Integrated Biosphere Model of Land Surface Processes, Terrestrial Carbon Balance, and Vegetation Dynamics. *Glob. Biogeochem. Cycle* **1996**, *10*, 603–628. [CrossRef]
26. Post, W.M.; Emanuel, W.R.; Zinke, P.J.; Stangenberger, A.G. Soil Carbon Pools and World Life Zones. *Nature* **1982**, *298*, 156–159. [CrossRef]
27. Zhang, X.S. A vegetation-climate classification system for global change studies in China. *Quat. Sci.* **1993**, *13*, 157–169, 193–196.
28. Fan, Z.M.; Fan, B. Shifts of the Mean Centers of Potential Vegetation Ecosystems under Future Climate Change in Eurasia. *Forests* **2019**, *10*, 873. [CrossRef]
29. Audebert, P.; Milne, E.; Schiettecatte, L.-S.; Dionisio, D.; Sinitambirivoutin, M.; Pais, C.; Proença, C.; Bernoux, M. Ecological Zoning for Climate Policy and Global Change Studies. *Nat. Sustain.* **2024**, *7*, 1294–1303. [CrossRef]
30. Jin, B.S.; Nie, M.; Li, Q.; Chen, J.K.; Zhou, W.B. Basic characteristics, challenges and key scientific questions of the Poyang Lake Basin. *Resour. Environ. Yangtze Basin* **2012**, *21*, 268–275.
31. Jian, Y.X.; Li, R.D.; Wang, J.B.; Chen, J.K. Aquatic plant diversity and remote sensing of the beach vegetation in Lake Poyang. *Chin. J. Plant Ecol.* **2001**, *25*, 581–587.
32. Gu, T.T.; Zhou, S.Q.; Shao, B.F.; Li, Q. Interactions between vegetation cover change and precipitation in Poyang Lake region. *Chin. J. Ecol.* **2009**, *28*, 1060–1066.
33. Li, X.H.; Zhang, Q.; Shao, M. Spatial and temporal variability of leaf area index in the Poyang Lake Basin and its relationship with climatic factors. *Resour. Environ. Yangtze Basin* **2012**, *21*, 296–301.
34. Yao, B.N.; Chen, B.Z.; Che, M.L. Spatial-temporal change of gross primary productivity in the Poyang Lake Basin from 2000 to 2013 and correlation with meteorologic factors. *Chin. Bull. Bot.* **2016**, *51*, 639–649. [CrossRef]
35. Yang, X.X. Impacts of Climate Change and Human Activities on the Terrestrial Vegetation Cover Changes in the Poyang Lake Basin. Master's Thesis, Southwest University, Chongqin, China, 2022.
36. Li, B.Z.; Wang, J.F.; Wang, H.Q.; Xia, L.J.; Su, R.; Dai, Z.J. Study on the Carbon Sink Value of Forest and Vegetation in Jiangxi Province. *Meteorol. Disaster Reduct. Res.* **2018**, *41*, 207–211. [CrossRef]
37. Wu, G.X.; Tang, X.J.; Ruan, H.H.; Luo, X.F. Carbon storage and carbon sequestration potential based on forest inventory data in Jiangxi Province, China. *J. Nanjing For. Univ. Nat. Sci. Ed.* **2019**, *43*, 105–110.
38. Yue, T.X. *Surface Modeling: High Accuracy and High Speed Methods*, 1st ed.; CRC Press: Boca Raton, FL, USA, 2017; ISBN 1-138-07567-1.
39. Yue, T.X.; Zhao, N.; Liu, Y.; Wang, Y.F.; Zhang, B.; Du, Z.P.; Fan, Z.M.; Shi, W.J.; Chen, C.F.; Zhao, M.W.; et al. A Fundamental Theorem for Eco-Environmental Surface Modelling and Its Applications. *Sci. China Earth Sci.* **2020**, *63*, 1092–1112. [CrossRef]
40. Gong, W.P.; Zhang, Q.; Fan, Z.M.; Shi, W.J.; Zhao, N.; Du, Z.P.; Yang, Y.; Chen, K.N.; Hu, J.X.; An, T.R.; et al. Future Scenarios of Forest Carbon Sink in a Typical Subtropical County. *Forests* **2024**, *15*, 1887. [CrossRef]
41. Whittaker, R.H. *Communities and Ecosystems*; Macmillan Company: London, UK, 1975.
42. Zhang, F.; Zhang, J.T.; Zhang, F. Pattern of forest vegetation and its environmental interpretation in Zhuweigou, Lishan Mountain Nature Reserve. *Acta Ecol. Sin.* **2003**, *23*, 421–427.
43. Yue, T.X.; Fan, Z.M.; Chen, C.F.; Sun, X.F.; Li, B.L. Surface Modelling of Global Terrestrial Ecosystems under Three Climate Change Scenarios. *Ecol. Model.* **2011**, *222*, 2342–2361. [CrossRef]
44. Cheng, W.M.; Zhou, C.H.; Chai, H.X.; Zhao, S.M.; Li, B.Y. Quantitative extraction and analysis of basic morphological types of land geomorphology in China. *J. Geo-Inf. Sci.* **2009**, *11*, 725–736. [CrossRef]

45. Xia, W.L. Spatio-Temporal Variation of NDVI and Its Relationship with Environmental Factors in Jiangxi Province. Master's Thesis, East China University of Technology, Jiangxi, China, 2017.
46. Belotelov, N.V.; Bogatyrev, B.G.; Kirilenko, A.P.; Venevsky, S.V. Modelling of Time-Dependent Biome Shifts under Global Climate Changes. *Ecol. Model.* **1996**, *87*, 29–40. [CrossRef]
47. Chen, X.W.; Zhang, X.S.; Li, B.L. The Possible Response of Life Zones in China under Global Climate Change. *Glob. Planet. Change* **2003**, *38*, 327–337. [CrossRef]
48. Szelepcsényi, Z.; Breuer, H.; Kis, A.; Pongrácz, R.; Sümegi, P. Assessment of Projected Climate Change in the Carpathian Region Using the Holdridge Life Zone System. *Theor. Appl. Climatol.* **2018**, *131*, 593–610. [CrossRef]
49. Fan, Z.M.; Bai, X.Y. Scenarios of Potential Vegetation Distribution in the Different Gradient Zones of Qinghai-Tibet Plateau under Future Climate Change. *Sci. Total Environ.* **2021**, *796*, 148918. [CrossRef]
50. Fan, Z.M. Dynamic Patterns of the Vertical Distribution of Vegetation in Heihe River Basin since the 1980s. *Forests* **2021**, *12*, 1496. [CrossRef]
51. Ye, C.; Liu, Y.B.; Zhao, X.S.; Wu, G.P. Analysis of Poyang Lake wetland vegetation growth dynamics and its response to lake water level based on MODIS. *Resour. Environ. Yangtze Basin* **2013**, *22*, 705–712.
52. Liu, T.T.; Yang, X.X.; Ye, X.C.; Wu, J.; Liu, J. Effects of human activities on terrestrial vegetation coverage change of Poyang Lake Basin during 2000–2020. *Bull. Soil Water Conserv.* **2022**, *42*, 320–329. [CrossRef]
53. Wu, Z.; Dai, E.F.; Lin, M.Z. Simulating the effect of climate change and human activities on the forest ecosystem in the hilly red soil region of southern China: A case study in Taihe county, Jiangxi province. *Geogr. Res.* **2018**, *37*, 2141–2152.
54. Liu, M.X.; Liu, Y.C.; Chen, M.; Li, Q.; Liang, Q.; Zou, J.P.; Qiaolipanguli, T.E.H. Spatiotemporal evolution of vegetation coverage and its response to climate change in upper reaches of Ganjiang river basin during 2000–2018. *Bull. Soil Water Conserv.* **2020**, *40*, 284–290. [CrossRef]
55. Lin, Y.B.; Wang, X.J.; Quan, M.Y.; Lin, D.R.; Lu, Y.; Liu, G.X. Spatiotemporal characteristics of vegetation coverage and its terrain gradient effect in Jiangxi and Fujian provinces in south China. *Res. Soil Water Conserv.* **2024**, *31*, 290–300. [CrossRef]
56. Sugden, A.; Smith, J.; Pennisi, E. The Future of Forests. *Science* **2008**, *320*, 1435. [CrossRef]
57. Song, Y.; Jin, L.; Wang, H.B. Vegetation Changes along the Qinghai-Tibet Plateau Engineering Corridor Since 2000 Induced by Climate Change and Human Activities. *Remote Sens.* **2018**, *10*, 95. [CrossRef]
58. Pan, Y.; Lin, J.; Tong, G.C.; Tang, P.; Zhang, J.C.; Gu, Z.Y. Spatio-Temporal Variations of Vegetation Coverage in Taihu Lake Basin From 2004 to 2014. *J. Ecol. Rural Environ.* **2018**, *34*, 37–45.
59. Liu, S.L.; An, N.N.; Yin, Y.J.; Cheng, F.Y.; Dong, S.K. Relationship Between Spatio-Temporal Dynamics of Soil and Water Loss and NDVI of the Small Basins in the Middle Reaches of Lancang River Based on SWAT Model. *J. Soil Water Conserv.* **2016**, *30*, 62–67. [CrossRef]
60. Mao, Z.Y.; Xu, L.G.; Lai, X.J.; Wang, X.L.; Li, Y.L.; Li, X.H.; Cai, Y.J.; Fan, H.X.; Wu, Y.K.; Wei, F.K. Assessment on ecosystem health of Lake Poyang based on a comprehensive index method. *J. Lake Sci.* **2023**, *35*, 1022–1036. [CrossRef]

Disclaimer/Publisher's Note: The statements, opinions and data contained in all publications are solely those of the individual author(s) and contributor(s) and not of MDPI and/or the editor(s). MDPI and/or the editor(s) disclaim responsibility for any injury to people or property resulting from any ideas, methods, instructions or products referred to in the content.